DYNA
http://dyna.medellin.unal.edu.co/

UNIVERSIDAD NACIONAL DE COLOMBIA

Influence of input variables on the unitary deformation experienced in pipes subjected to the action of lateral loads

Julián Francisco Gamba-Gómez [a], Yaneth Pineda-Triana [a], Daniel Mauricio Bermúdez-Rincón [a] & Osmar Albert Gamba-Gómez [b]

[a] *Facultad de Ingeniería, Universidad Pedagógica y Tecnológica de Colombia, Tunja, Colombia. julian.gamba@uptc.edu.co, yaneth.pineda@uptc.edu.co, daniel.burmudez01@uptc.edu.co*
[b] *Facultad de Ciencias y Tecnología, Universidad Santo Tomas, Bogotá, Colombia. osmar.gamba@usta.edu.co*

Received: October 6th, 2023. Received in revised form: February 9th, 2024. Accepted: March 14th, 2024.

Abstract
The hydrocarbon transportation industry uses extensive pipeline networks subject to complex loading conditions. The finite element analysis (FEA) has proven to be effective in simulating the deformation behavior in these pipelines, which assists in the assessment of their integrity and risks. In this work, a model developed using finite elements is proposed to analyze the behavior of API 5L Gr B carbon steel pipes, subject to internal pressure and lateral loads. The model is validated through uniaxial tensile and four-point bending tests. In addition, parametric analysis is carried out considering variables such as diameter, lateral load, and distance between supports. The objective is to identify which one of these variables has the most influence in the unit strain. The results indicate that the unit strain obtained from the numerical model agrees with the experimental tests. Furthermore, it is concluded that the diameter is the influential parameter.

Keywords: pipelines; bending moment; risk assessment; integrity pipeline.

Influencia de las variables de entrada en la deformación unitaria evidenciada en tuberías sometidas a la acción de cargas laterales

Resumen
La industria del transporte de hidrocarburos utiliza extensas redes de tuberías sometidas a condiciones de carga complejas. El análisis por elementos finitos ha demostrado ser efectivo para simular el comportamiento de deformación en estas tuberías, lo que ayuda en la evaluación de su integridad y riesgos. En este trabajo, se propone un modelo desarrollado mediante elementos finitos para analizar el comportamiento de tuberías de acero al carbono API 5L Gr B, sujetas a presión interna y cargas laterales. El modelo se valida mediante pruebas experimentales de tensión y flexión de cuatro puntos. Además, se realiza análisis paramétrico considerando variables como diámetro, la carga lateral y distancia entre soportes. El objetivo es identificar cuál de estas variables influye más en la deformación unitaria. Los resultados indican que la deformación unitaria obtenida del modelo numérico concuerda con las pruebas experimentales. Además, se concluye que el diámetro es el parámetro influyente.

Palabras clave: tuberías de transporte; momento flector; evaluación de riesgo; integridad de tuberías.

1 Introduction

Hydrocarbon transportation pipelines are one of the most economical means used to carry out this type of activities [1] (ASME, 2010). Due to the flexibility during the construction process, it is common to manufacture transportation networks that extend over large lengths [2] (Ellenberger, 2010), crossing different geographies during its transit that can range from flat terrain to undulating and high mountain terrain. Due to the heterogeneity in geography, it is common for lines to be subjected to complex vertical, lateral, and axial load conditions added to the internal pressure used for transportation [3] (Ozkan & Mohareb, 2009), these loads can generate unplanned deformations in the pipes. It is estimated that about 23% of the failures that have occurred in pipelines in the United States in the last 20 years are associated with these types of loads [4] (Ahn et al., 2016).

How to cite: Gamba-Gomez, J.F., Pineda-Triana, Y., Bermudez-Rincon, D.M. and Gamba-Gomez, O.A., Influence of input variables on the unitary deformation experienced in pipes subjected to the action of lateral loads. DYNA, 91(232), pp. 33-40, April - June, 2024.

The application of lateral and axial loads in pipes can generate local collapse of the structure [5] (Bazhenov et al., 2016), this behavior depending on the characteristics of the phenomenon and the function for which the component is intended, can compromise its structural capacity (Li et al., 2017), generating damage such as wrinkles, ovals, and cracks among others [6] (Antaki, 2005).

It has been shown that the diameter and magnitude of the applied load are some of the parameters that influence the result of strain and stress experienced by the material [3] (Ozkan et al., n.d.), these parameters being of interest for the operation, design and integrity management [1] (ASME, 2010) sites in which environmental conditions occur that facilitate the application of external loads.

The finite element technique (FEA) in which plastic behaviors of the material are included is suitable for simulating pipes subjected to various loading situations [7] (Cai et al., 2018), it is important to emphasize that when large deformations occur, the material hardening model must consider strain hardening [4] (Ahn et al., 2016), whether general or local.

The present work proposes a numerical model based on the finite element technique, which considers non-linear behaviors in terms of material, geometry, and contacts. The objective of the analysis focuses on taking as input parameters the diameter of the pipe, the magnitude of the applied load and the distance between supports and evaluating which of them has the greatest impact on the unit strain results obtained.

The proposed FEA model is validated through uniaxial tension and four-point bending results. The identification of the relevance of parameters is carried out through the development of an experimental design, based on the response surface technique, which takes as input data the results obtained from the FEA model for the sample points defined in the experimental design.

2 Materials and methods

For the development of the FEA model, the ANSYS v 2023 R2 software in its academic version was used. The developed model uses 3D type elements to perform the discretization, considering nonlinearities of the material type, contacts, and geometry, in order to reduce the computational cost of the solution, it was contemplated to evaluate a quarter of the geometry, including symmetry conditions in the X and Z axes for this purpose. As strategies for stabilization and convergence of the solution, low-stiffness springs were included and the number of loading steps and substeps was adjusted [8] (Nazemi, 2009).

2.1 Finite element model

The developed FEA model considers the geometry used during a four-point bending test [16], including the pipe under analysis, a set of rollers that supports the pipe and another that applies the load. The length of the pipe considered was 6 times the diameter of the pipe, with a view to avoid the end effect.

For the discretization of the model, solid elements of the SOLID 186 type [9] (ANSYS, 2022b) were used. These elements allow six degrees of freedom and within their formulation they consider the effects of nonlinearities associated with material, contacts, and geometry.

The numerical model developed considered a mapped type of mesh with refinements in the load application zones and boundary conditions. The mesh used included a total of 24,884 nodes associated with 4,364 elements. In order to guarantee the results obtained are independent of the discretization used, skeweness was used as a metric, obtaining values of 0.004826 m the worst case.

2.2 Loading and boundary conditions

The load application was carried out through two steps (Li et al, 2017) (Wang et al, 2021) [10,11], the first step considers the application of a pressure of 8.27 Mpa on the internal face of the pipe , together with the displacement in the -Y direction of the load application roller, the second step considers the application of a displacement in the +Y direction of the load application roller, which frees the pipe from the action of the lateral load.

As a boundary condition, a Fixed support type constraint [12] (ANSYS, 2022a) was applied to the load support roller. This condition does not allow the displacement or rotation of any degree of freedom. The constraint remained constant during the two load application steps (Shuai et al, 2020) [13]. In order to facilitate the convergence of the model, low stiffness springs were included during all load application steps.

2.3 Material parameters

The material used considers the properties of an API 5L Gr B steel, under a multilinear type of isotropic hardening model [14] (Kamaya, 2014), the stress-strain data considered were taken from tests of tension carried out on specimens made of this material. To assure the behavior of the material fits the input data, tests were carried out in the software considering the same geometry of the tension test (Tee, 2020) [15].

2.4 Model Calibration

Model validation was carried out using the results of a four-point bending test, the geometry considered for the development of the tests [16] is presented in Fig 1. The simulation point selected to validate the model corresponded to a pipe diameter of 0.1016 m, lateral displacement of 0.09 m, distance between supports of 0.6 m, thickness of 0.003048 m, and API 5L Gr B carbon steel, the axial deformation at the point indicated in Fig 2 was considered as the output variable. The selection of the values for the validation point considered the ease of acquiring the material for the manufacture of the specimens, characteristics of the equipment available in the laboratory and typical configurations found in hydrocarbon distribution networks.

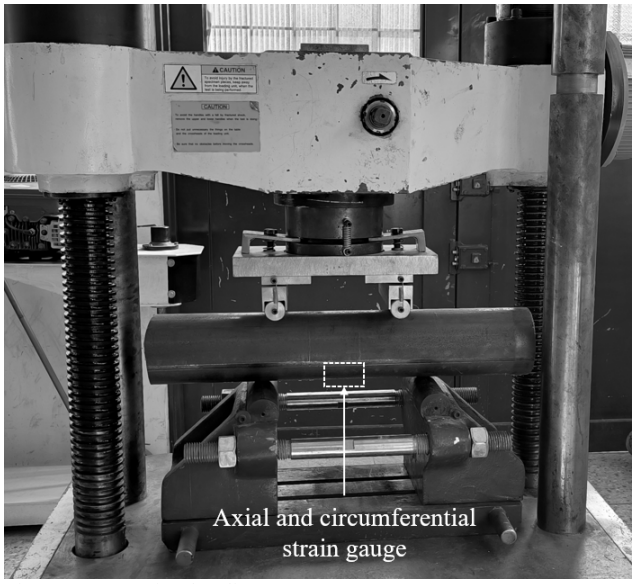

Figure 1. Four points bending-test
Source: The author

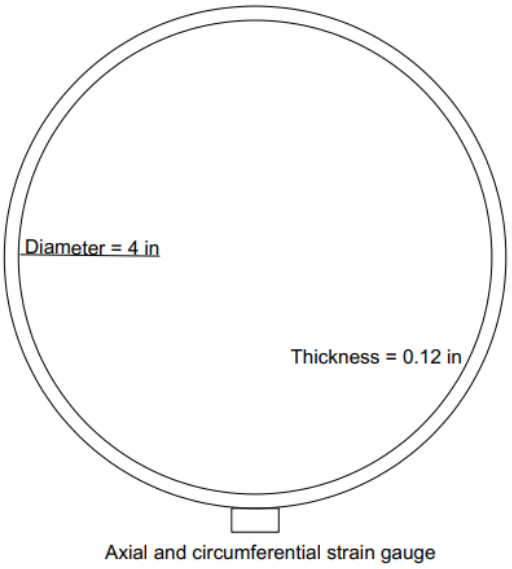

Figure 2. Deformation measurment configuration
Source: The author

The output graphs are expressed in terms of lateral displacement vs evidenced deformation, in each of the positions described in Fig 2.

The deformation measurements were carried out using a deformation measurement device, the assembly was built with two (2) type K strain gauges, one for the measurement of the circumferential strain and another for the measurement of the axial strain, as presented in the Figs. 2, 3.

The electronic device for measuring deformation includes a Wheaston bridge, coupled to a Raspberry 4.0 card to capture, store, and process the information coming from the gauges. This information is stored and presented through an interface developed in Python. The developed scheme is presented in Figs. 3 and 4.

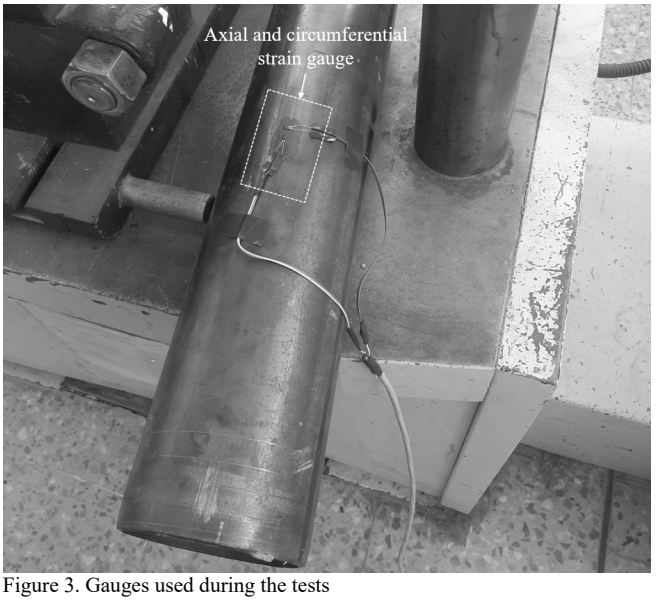

Figure 3. Gauges used during the tests
Source: The author

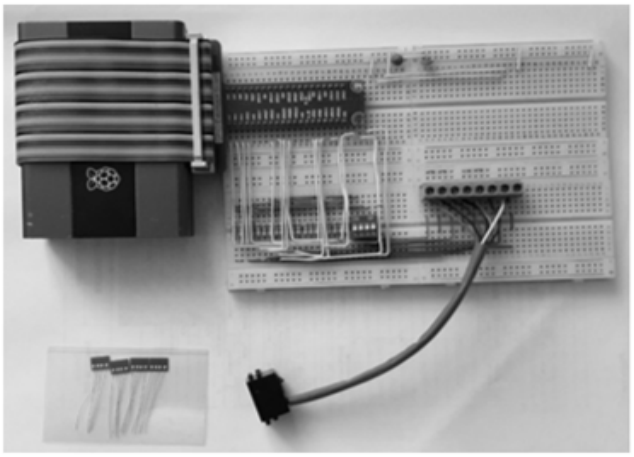

Figure 4. Electronic Setup to obtained signal from sensors
Source: The author

The measuring device was calibrated through tension tests carried out on a Shimadzu UH500 KNI universal machine, in which a flat probe 40 cm long, 2 cm wide and 0.30 cm thick and a load application speed of 5 mm/minute were placed [17]. A strain gauge was placed in the specimen to measure the deformation in the direction of load application in parallel with the extensometer Shimadzu TYPE STRAIN SG 50 – 50. To have additional data to perform the numerical validation of the model, the test described above was developed using a numerical model, in which the geometry was developed and meshed using the same type of solid elements and considering the same material model, graphs of the test setup and its numerical equivalent are presented in Fig 5.

From the graphs obtained, it can be seen how the results obtained from the numerical model are consistent with those reported in the experimental test, which allows the validation of the developed model.

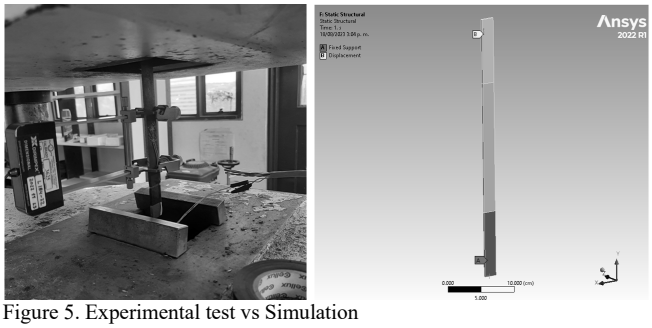

Figure 5. Experimental test vs Simulation
Source: The author

Table 1.
Experimental design range.

Diameter V1 [m]	0.0508	0.1016	0.2032
Lateral Distance V2 [m]	0.03	0.06	0.09
Axial Distance V3 [m]	0.3	0.45	0.6

Source: The author

2.5 Experiment design

In order to analyze which of the geometric parameters is most relevant when bending deformation phenomena occur, the following variables of interest were selected for the present study: magnitude of the applied lateral load, distance between the supports and diameter of the pipe. From these variables, an experimental design of the response surface type was carried out, having the values described in Table 1 for each of the variables.

The ranges of the variables presented were selected to obtain output data that are in the plastic zone of the material, without reaching the ultimate breaking stress, this so that the output data can be used to make comparisons with real pipeline operation cases. In addition to this, there was a maximum distance of 10 cm as a restriction for lateral displacement, due to the support available for the execution of the four-point bending test.

3 Results

3.1 Model validation

The model validation results are presented for the tensile test and the result of the four-point bending test.

3.1.1 Tensile test results

The Fig 6 shows the deformation results obtained for the tension test and the respective numerical model. The graph shows how the two results present similar linear behaviors. It is important to indicate that a slight difference is seen in the results of stress in the area close to the yield stress, this is because the model considers the local plasticization phenomenon that can occur once the proportional limit is exceeded, forming transient Luder's bands [18].

The curve presented in Figure 6 was constructed from the displacement and force data measured in the universal machine, as described in eq. (1)(2), these values are transformed into true stress and deformation according to eqs. (3)(4).

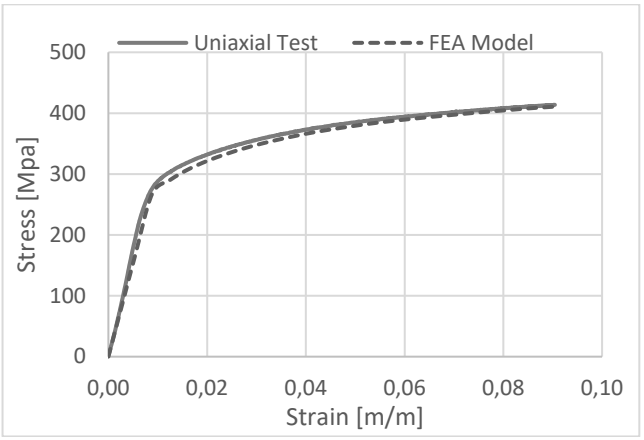

Figure 6. Deformation Test vs Numerical Model
Source: The author

$$\sigma_{Eng} = \frac{F}{A_{Ini}} \quad (1)$$

$$\varepsilon_{Eng} = \frac{\Delta L}{L_{Ini}} \quad (2)$$

$$\sigma_{real} = \sigma_{Eng} * \left(1 + \varepsilon_{Eng}\right) \quad (3)$$

$$\epsilon_{real} = ln\left(1 + \varepsilon_{Eng}\right) \quad (4)$$

Where σ_{Eng}, ε_{Eng} correspond to the engineering stress and deformation, σ_{real} and ϵ_{real} correspond to the real stress and deformation.as well as A_{Ini} and L_{Ini} correspond to the area and initial lengths of the specimens.

In the case of the numerical model developed using the finite element technique, it calculates the displacements according to eq. (5)

$$F = K * u \quad (5)$$

Where F corresponds to the external force matrix, K to the global stiffness matrix of the structure and u corresponds to the nodal displacement matrix. For cases in which there are non-linearities; Whether geometric, contact or material, the stiffness matrix is not constant and varies with displacement, the solution of this type of systems is obtained through an iterative series of linear approximations.

3.1.2 Four-point bending test results

The Fig 7 presents the configuration of the numerical model, loads and restrictions, and Fig. 8 describes the location of the point for deformation measurement.

The comparison between the results of the numerical model and those obtained from the experimental setup are presented in Fig. 9. In the case of the experimental results, the curve presented was constructed from the data of lateral displacement vs longitudinal deformation measured by the strain gauges, these same quantities were taken from the numerical model. It is important to mention that the quantities described were selected, taking into account that they are the primary data obtained from the sensors installed during the test execution.

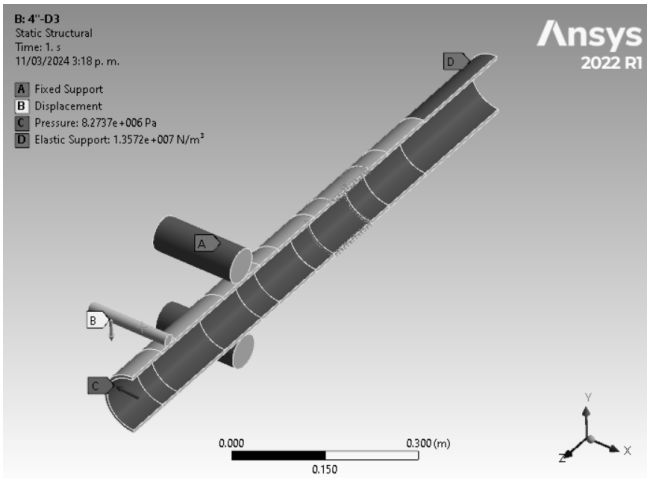

Figure 7. Numerical model configuration
Source: The author

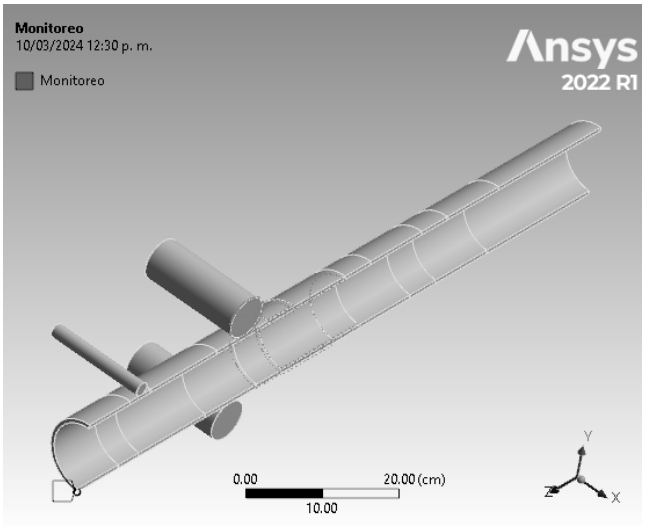

Figure 8. Deformation measurement point
Source: The author

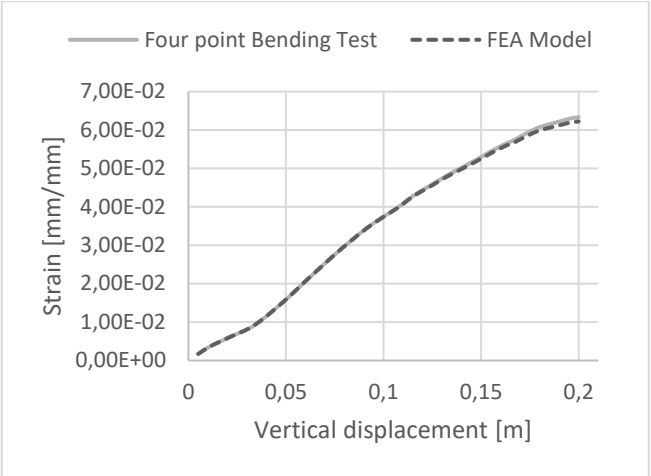

Figure 9. Unitary Deformation
Source: The author

From the results obtained, a similar behavior can be seen in both cases. This observation allows us to corroborate the coherence between the results, thereby validating the behavior of the numerical model [23-25]. During the development of the analysis, it was evident that the maximum error does not exceed 7% and this is in the middle region of the plasticity zone, the difference between the numerical values and the experimental ones in this zone can be associated with the capacity of deformation of the adhesive used to fix the gauges to the base metal [21], which can have a lower deformation rate than that of the base metal, especially for considerable deformations.

3.2 Experimental design results

The results obtained from the FEA numerical model for the four-point bending test, considering the variables, ranges and nomenclature defined in Table 1, are presented in Table 2 in terms of strain (E1) and principal stress (S1). From the data presented, it can be seen the ultimate tensile strength of the material was not exceeded considering the limit values defined in API 5L for a Gr B steel [20] (API, 2013).

When verifying the results presented in Table 2, it can be seen how the highest stress results are presented for diameters of 0.0508 m, with values close to 339.8 Mpa, this value is above the yield point of the material (248 Mpa) [20] (API,2013) but well below the ultimate tensile strength of the material (415 Mpa)[20](API,2013), for the case of 0.1016 m the stress is reduced on average by about 10%, presenting a similar behavior with respect to the yield limits and ultimate strength described. Finally, the lowest stress occurred for diameters of 0.2032 m which the average value is very close to the yield limit of the material. The stress and deformation results presented correspond to real values.

Table 2.
Principal Strain and Stress.

V1 [m]	V2 [m]	V3 [m]	E1 [m/m]	S1 [MPa]
0.0508	0.03	0.3	1.67E-03	333.7
0.0508	0.03	0.45	1.66E-03	332.5
0.0508	0.03	0.6	1.64E-03	327.6
0.0508	0.06	0.3	1.69E-03	338.1
0.0508	0.06	0.45	1.70E-03	339.0
0.0508	0.06	0.6	1.68E-03	336.6
0.0508	0.09	0.3	1.67E-03	333.7
0.0508	0.09	0.45	1.70E-03	339.7
0.0508	0.09	0.6	1.70E-03	339.8
0.1016	0.03	0.3	1.43E-03	285.4
0.1016	0.03	0.45	1.61E-03	321.7
0.1016	0.03	0.6	1.65E-03	329.3
0.1016	0.06	0.3	1.51E-03	301.1
0.1016	0.06	0.45	1.67E-03	333.9
0.1016	0.06	0.6	1.71E-03	341.9
0.1016	0.09	0.3	1.52E-03	304.7
0.1016	0.09	0.45	1.66E-03	332.4
0.1016	0.09	0.6	1.72E-03	344.4
0.2032	0.03	0.3	3.11E-04	62.2
0.2032	0.03	0.45	5.45E-04	109.0
0.2032	0.03	0.6	7.49E-04	149.8
0.2032	0.06	0.3	1.02E-03	204.5
0.2032	0.06	0.45	1.25E-03	250.8
0.2032	0.06	0.6	1.39E-03	278.6
0.2032	0.09	0.3	1.49E-03	297.8
0.2032	0.09	0.45	1.62E-03	323.7
0.2032	0.09	0.6	1.66E-03	331.9

Source: The author

Table 3.
ANOVA results

Source	DF	Adj SS	Adj MS	F-Value	P-Value
Model	6	0.000003	0.000001	44.58	0
Linear	3	0.000003	0.000001	69.41	0
V1[m]	1	0.000002	0.000002	125.97	0
V2[m]	1	0.000001	0.000001	69.23	0
V3[m]	1	0	0	13.02	0.002
2-Way Int	3	0.000001	0	25.92	0
V1[m]*V2[m]	1	0.000001	0.000001	71.66	0
V1[m]*V3[m]	1	0	0	5.76	0.026
V2[m]*V3[m]	1	0	0	0.34	0.567
Error	20	0	0		
Total	26	0.000004			

Source: The author

To establish in greater detail, the relevance of the factors considered together with their interaction, ANOVA analysis was carried out on the results obtained. The analysis data are presented in Table 3, having a significance level of the test of 0.05.

For the data presented, the quantity Adj SS corresponds to the sum of squares, Adj MS corresponds to the sum of the mean square, F-Value corresponds to the statistic of a Fisher test, understood as the variance between the measurement of the samples/variation within of the samples and P-Value corresponds to the probability of obtaining a value equal to or greater than the one observed [22].

From the data presented in Fig. 9 and Table 3, it can be seen the parameter that has the greatest relevance on the principal strain value obtained is the diameter of the pipe. Likewise, it was evident that the interaction between the diameter and the magnitude of the lateral displacement is the second most relevant factor the lateral displacement as the third factor and distance between supports as fourth factor. It is important to mention that both the interaction and the magnitude of the lateral displacement have similar orders of magnitude. Finally, the combination of diameter/distance between supports is the interaction with the least relevance, the interaction between the magnitude of the lateral load and the distance between supports has no significant relevance in the strain result.

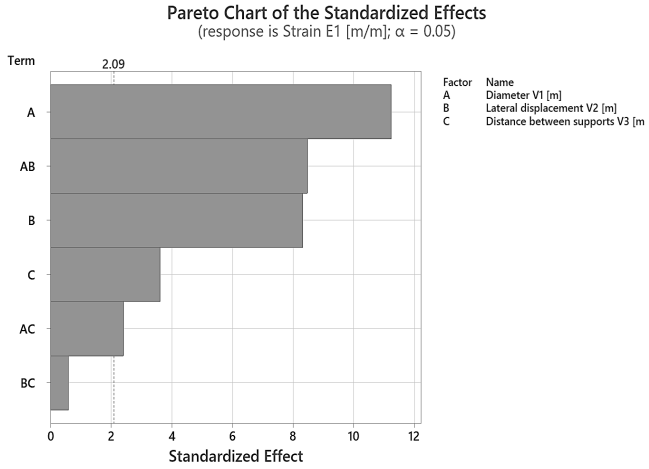

Figure 9. ANOVA results
Source: The author

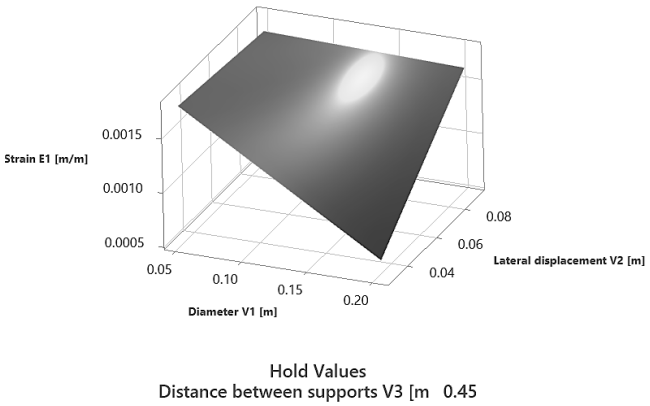

Figure 10. Strain as diameter and lateral displacement
Source: The author

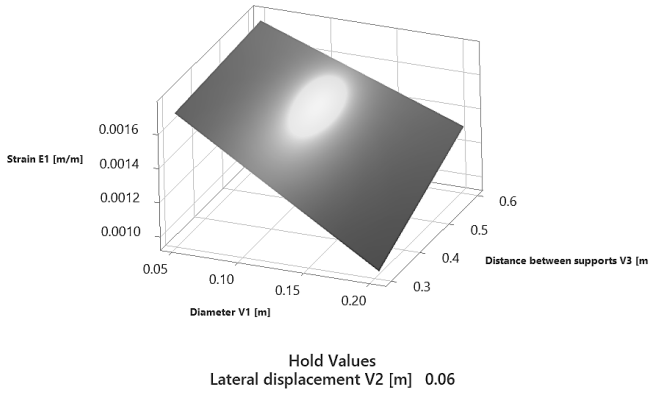

Figure 11. Strain as function of diameter and lateral desplacement
Source: The author

The Fig. 10 shows the response surface obtained for the strain as a function of the diameter of the pipe and the magnitude of the lateral displacement. In the Figure it can be seen how the lowest strain values are obtained for larger diameters and low magnitudes of lateral displacement, the magnitude of the strain increases as the diameter decreases and the lateral displacement increases, the influence on the strain result being more representative for increases in diameter. Likewise, a quadratic behavior can be seen in the strain result as the two parameters increase simultaneously.

Regarding the behavior of the effort when the diameter of the pipe and the distance between supports are taken as input parameters, the response surface obtained is presented in Fig. 11, a linear behavior in the growth of the effort was evident as the diameter decreases and the distance between supports increases, the interaction between the two input parameters exhibits linear behavior for the entire range of values considered.

Finally, the behavior of the principal strain as a function of the lateral displacement and the distance between supports is presented in T 12, in which linear increases in the strain can be seen as the input parameters are varied. In this case, it is important to mention that the relevance of the interaction between the input parameters is not significant.

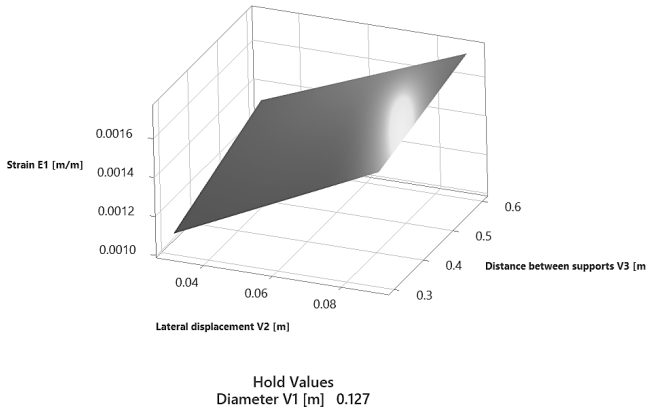

Figure 12. Stress as function supports and lateral displacement
Source: The author

4 Conclusions

The present analysis studies the influence of factors such as the diameter of the pipe, the magnitude of the applied transverse load and the distance between supports on the level of strain that can be evidenced in a pipe. A numerical model was developed using the finite element technique to analyze the phenomenon; the results were validated through experimental uniaxial tension and four-point bending tests. Finally, on the validated model, an experimental design of the response surface type was defined, in which each of the input variables were varied in three ranges and the results were obtained in terms of principal stress and strain, the most relevant conclusions are presented below.

The results obtained from the numerical model developed using 3D solid elements to discretize the geometry are in good agreement with the results obtained for both the uniaxial tension test and the four-point bending test. This allows the technique to be used to analyze the behavior that a pipe can experience when it is subjected to bending moments.

Of the variables considered, the diameter is the one that has the greatest relevance when a pipe is subjected to a lateral load, in the same way the magnitude of lateral displacement is the second independent variable that influences the result of strain obtained, finally the distance between supports is the last variable with significant relevance to the strain result obtained.

Regarding the interactions between the variables, it was evident that the interaction between the diameter of the pipe/magnitude of the lateral displacement is the most relevant, exhibiting a quadratic growth in the strain as the diameter decreases and the lateral load increases simultaneously. The second interaction of relevance is the one that occurs when the diameter and distance between supports vary simultaneously; however, this effect is low and is very close to the limit of significance. Finally, the interaction between the magnitude of the lateral displacement and the distance between supports does not have significant relevance in the strain result obtained.

Regarding the measurement of deformation using strain gauges, it was evident that in general terms these allow for an adequate measurement; it is important to take care of the effect of temperature on this type of device since it can significantly impact the result obtained.

References

[1] ASME, Pipeline Integrity Assurance-A Practical Approach, [Online]. 2010. Available at: https://www.copyright.com
[2] Phillip, J., Ellenberger, Piping and pipeline calculations manual: construction, design, fabrication, and examination. Butterworth-Heinemann/Elsevier, 2010.
[3] Ozkan, I.F., Mohareb, M. and Asce, M., Testing and Analysis of Steel Pipes under Bending, Tension, and Internal Pressure, Journal of Structural Engineering, 135(2), art. 9445, 2009. DOI: https://doi.org/10.1061/(ASCE)0733-9445(2009)135:2(187).
[4] Ahn, K., Lim, I.G., Yoon, J., and Huh, H., A simplified prediction method for the local buckling load of cylindrical tubes, International Journal of Precision Engineering and Manufacturing, 17(9), pp. 1149–1156, 2016. DOI: https://doi.org/10.1007/s12541-016-0139-0.
[5] Bazhenov, V.A., Luk'yanchenko, O.O., Kostina, O.V., and Gerashchenko, O.V., Nonlinear bending stability of a long flexible cylindrical shell with geometrical imperfections. Strength of Materials, 48(2), pp. 308–314, 2016, DOI: https://doi.org/10.1007/s11223-016-9766-z.
[6] Antaki, G.A., Fitness-for-service and integrity of piping, vessels, and tanks: ASME code simplifed. McGraw-Hill, USA, 2005.
[7] Cai, J., Jiang, X., Lodewijks, G., Pei, Z., and Wu, W., Residual ultimate strength of seamless metallic pipelines under a bending moment-a numerical investigation, Ocean Engineering, 164, pp. 148–159, 2018. DOI: https://doi.org/10.1016/j.oceaneng.2018.06.044.
[8] Nazemi, N., Behavior of X60 Line Pipe under Combined Axial and Transverse Loads with Internal Pressure, 2009. [Online]. Available at: https://scholar.uwindsor.ca/etd
[9] ANSYS, Element Reference, 2022. [Online]. Available at: http://www.ansys.com
[10] Li, Y., Shuai, J., Jin, Z.L., Zhao, Y.T., and Xu, K., Local buckling failure analysis of high-strength pipelines, Pet Sci, 14(3), pp. 549–559, 2017. DOI: https://doi.org/10.1007/s12182-017-0172-3.
[11] Wang, J., Shuai, Y., He, R., Dou, X., Zhang, P., and Feng, C., Ultimate strain capacity assessment of local buckling of pipelines with kinked dents subjected to bending loads. Thin-Walled Structures, 169, 2021. DOI: https://doi.org/10.1016/j.tws.2021.108369.
[12] ANSYS, Basic Analysis Guide, 2022. [Online]. Available at: http://www.ansys.com
[13] Shuai, Y. et al., Local buckling failure analysis of high strength pipelines containing a plain dent under bending moment, J Nat Gas Sci Eng, 77, 2020, DOI: https://doi.org/10.1016/j.jngse.2020.103266.
[14] Kamaya, M., Ramberg-Osgood type stress-strain curve estimation using yield and ultimate strengths for failure assessments, International Journal of Pressure Vessels and Piping, 137, pp. 1–12, 2014. DOI: https://doi.org/10.1016/j.ijpvp.2015.04.001.
[15] Tee, K.F., and Wordu, A.H., Burst strength analysis of pressurized steel pipelines with corrosion and gouge defects, Eng Fail Anal, 108, 2020 DOI: https://doi.org/10.1016/j.engfailanal.2019.104347.
[16] NACE, Standard Test Method - Four-Point Bend Testing of Materials for Oil and Gas Applications, 2016.
[17] ASTM E 8M, Standard Test Methods for Tension Testing of Metallic Materials, 2001.
[18] Han, J., Lu, Ch., Wu, B., Li, J., Li, H., Lu, Y., and Gao, Q., Innovative analysis of Luders band behaviour in X80 pipeline steel Materials Science & Engineering A, A683, pp. 123-128, 2017. DOI: https://doi.org/10.1016/j.msea.2016.12.008
[19] Urriolagoitia-Sosa, G., Durodola, J.F., Lopez-Castro, A., and Fellows, N.A., A method for the simultaneous derivation of tensile and compressive behaviour of materials under Bauschinger effect using bend tests, Journal of Mechanical Engineering Science, 220(10), pp. 1509-1518, 2006. DOI: https://doi.org/10.1243/09544062JMES180
[20] API Specification 5L, Specification for line pipe, 2013.
[21] Keil, S., Technology and practical use of strain gages, Publisher: Ernst & Sohn a Wiley Brand, 2017.
[22] Montgomery, D.C., Design and analysis of experiments, Wiley, USA, 2020.

[23] Shuai, Y. Wang, X-H., Cheng, Y.F., Buckling resistance of an X80 steel pipeline at corrosion defect under bending moment. J. Nat Gas Sci Eng, 93, art. 104016, 2021. DOI: https://doi.org/10.1016/j.jngse.2021.104016
[24] Wang, J. et al., Ultimate strain capacity assessment of local buckling of pipelines with kinked dents subjected to bending loads. J. Thin-Walled Structures, 169, art. 108369, 2021. DOI: https://doi.org/10.1016/j.tws.2021.108369
[25] Jindra, D. et al., Experimental and numerical simulation of a three-point bending test of a stainless-steel beam. J. Transportation Research Procedia, 55, pp. 1114-1121 2021. DOI: https://doi.org/10.1016/j.trpro.2021.07.183

J.F. Gamba-Gomez, received the BSc. Eng in Electromechanical Engineering in 2010, Postgraduate in Structural Numerical Analysis using the finite element method in 2019 from the ESSS, Postgraduate in numerical analysis of flows using CFD in 2020 from the ESSS and MBA Sp. in Business Intelligence and Big Data in 2020 from the European Postgraduate Institute. From 2012 to date she has worked as a stress and mechanical integrity analyst for different industries in the Oil & Gas sector. His research interests include: Structural simulation using finite elements; transient analysis using explicit dynamics; behavior of materials and analysis of technological risks in the operation of facilities used for the transportation of hydrocarbons.
ORCID: 0009-0008-8123-8147

Y. Pineda-Triana, received the BSc. Eng in Metallurgical Engineering in 1991, a Sp. in Industrial Radiography in 1993 from the Universidad Pedagógica y Tecnológica de Colombia and a Dr. in Mechanical and Materials Engineering from the Universidad Politécnica de Valencia, Spain. Currently, she is a full professor in the Engineering Metallurgical School at pregraduate and postgraduate level, Facultad de Ingeniería, Universidad Pedagógica y Tecnológica de Colombia. His research interests include: composites (laminates, reinforced plastics, synthetic and natural fibers); coatings and films; ceramics; mechanical engineering; process engineering.
ORCID: 0000-0002-5561-9412

D.M. Bermúdez-Rincón, received the BSc. Eng in Mechanical Engineering Engineer in 2015, from the Libre University. Bogotá, Colombia. Sp. in Integrity and Corrosion Management in 2019 from the Universidad Pedagógica y Tecnológica de Colombia, Tunja, Colombia. Since 2015 he has worked for companies in the Oil and Gas sector. He is currently a master's student in Integrity and Corrosion Management at the Universidad Pedagógica y Tecnológica de Colombia. His research interests include: simulation; modeling; mechanical integrity and risk analysis for hydrocarbon transportation pipelines
ORCID: 0009-0003-6045-7096

O.A. Gamba-Gómez, received the BSc. Eng in Civil Engineering in 2009 and a MSc. in Metallurgy and Materials Science in 2020, both from the Universidad Pedagógica y Tecnológica de Colombia, Tunja, Colombia. From 2010 to 2013 he worked in the private sector in the civil works sector, since the end of 2014 he has been working for the Universidad Pedagógica y Tecnológica de Colombia as an operative technician for the materials and structures laboratory, he was a professor for the civil engineering school in 2016, 2017 and 2021 in the undergraduate modality, he has also been a professor for the Specialization program in Construction Pathology at the Universidad Santo Tomas since 2022. His research interests include: new materials; mechanical testing; dynamic testing; advanced concrete design.
ORCID: 0000-0002-2124-5723